동맥 유동해석을 위한 스펙트럴 요소의 개발
Spectral Element Modeling for the Blood Flow through Artery

장인준† ·서보성*·이우식**
Injoon Jang, Bosung Seo and Usik Lee

Key Words : Blood vessel, Spectral finite element model, Blood pressure, Blood flow rate

ABSTRACT

As the blood flow characteristics have been recognized to be closely related to various cardiovascular diseases, it is very important to predict them accurate enough in an efficient way. Thus, this paper proposes a one-dimensional spectral finite element model for the human blood vessels. The spectral finite element model is formulated in the frequency-domain by using the exact frequency dependent shape functions and applied to an ascending aorta.

1. Introduction

The blood flow characteristics determine the wall shear stress and wall tension. As the wall shear stress and wall tension are closely related to the cardiovascular diseases such as stenosis and aneurysm, it is very important to predict the blood flow characteristics accurately in an efficient way for the cardiovascular disease research, medical devise design and surgical planning. To this end, computational methods have merged as the powerful tools for the modeling and analysis of the blood flow and pressure in arteries.

Modeling of blood flow and pressure has been studied intensively over the years, and various computational models have been reported in the references [1-8]. The one-dimensional (1D) models have been widely used because they can provide clinically relevant information on local mean blood flow and pressure waves through arterial systems very efficiently as well as the boundary conditions suitable for three-dimensional (3D) models [7, 8]. For solving 1D models of blood flow, the two-step Lax-Wendroff method [3] and finite element method (FEM) [4-6] have been applied in the literature. Though FEM is a very powerful tool for solving diverse complex engineering problems, it is often inevitable to use very fine meshes to get improved analysis results, which drastically increases the computation cost. In contrast to conventional FEM, the spectral finite element method (SFEM) [9] is known as an exact element method in which exactly formulated frequency-dependent shape functions are used to formulate the spectral finite element models. Thus, in SFEM, one can get exact dynamic behavior of a 1D continuum system by modeling the whole uniform parts of continuum system as the single finite elements, regardless of their length. This may benefit us to drastically reduce the computation cost. This motivates this study to apply the SFEM to the modeling and analysis of the blood flows through human blood vessels.

† 인하대학교 대학원 기계공학과
* 인하대학교 대학원 기계공학과
** 연락저자, 인하대학교 기계공학과 교수
E-mail : ulee@inha.ac.kr
Tel : (032) 860-7318, Fax : (032) 866-1434

2. Governing Equation

The 1D theory of arterial flow consists of a continuity equation, an axial momentum balance equation, and a constitutive equation for the flow in an impermeable, deforming, elastic domain as [2, 3]

$$\begin{aligned} &\dot{S} + Q' = 0, \\ &\dot{Q} + (1+\delta)\left(Q^2/S\right) + (A/\rho)P' \\ &\quad = vH(Q/S) + vQ'', \\ &P(S(x,t),x,t) \\ &\quad = P_d + (4/3)\left(Eh/r_d(x)\right)\left(1-\sqrt{S_d(x)/S(x,t)}\right) \end{aligned} \tag{1}$$

where S is the cross-sectional area, Q is the volumetric flow rate, P is the pressure, ρ is the mass density of blood, v is the kinematic viscosity of blood, E is the Young's modulus of artery, and h is the wall thickness of artery. $S_d(x)$ and $r_d(x)$ are the cross-sectional area and radius at diastole pressure P_d = 80 mmHg. The parameters δ and H are determined by the flow velocity profile over the cross-section of artery [2, 3]. Notice that the dot and the prime represent the derivative with respect to time t and coordinate x, respectively.

Assume that the blood pressure and cross-sectional area can be written as

$$S(x,t) = S_d(x) + s(x,t), \quad P(x,t) = P_d + p(x,t) \tag{2}$$

where S_0 is the cross-sectional area at the inlet of an artery and θ is a parameter representing the taper of an artery. By substituting Eq. (2) into Eq. (1) and using the assumption $S_d(x) = S_0(1-\theta x) > s(x, t)$, we can obtain the approximated continuity and momentum equations as

$$a_0 \dot{p} + a_1 Q' = 0,$$
$$a_0 p' + \dot{Q} + a_2 Q - a_3 Q'' = f(x,t) \tag{3}$$

where

$$f(x,t) = -a_4 Q^2 - a_5 Q Q' + a_6 p Q - a_7 p' p + a_8 p Q Q' + a_9 p Q^2 + a_{10} p' Q^2 \tag{4}$$

and

$$\begin{aligned} &a_0 = S_0/\rho\rho \; a_1 = \alpha/\rho, \; a_2 = \nu H/S_0, \\ &a_3 = \nu, \; a_4 = (1+\delta)\theta/S_0, \; a_5 = 2(1+\delta)/S_0, \\ &a_6 = \nu H/(\alpha S_0), \; a_7 = S_0/(\alpha\rho), \\ &a_8 = 2(1+\delta)/(\alpha S_0), \; a_9 = (1+\delta)\theta/(\alpha S_0), \\ &a_{10} = (1+\delta)/(\alpha S_0), \\ &\alpha = (2/3)\left[k_1 exp(k_2 r_d(x_c)) + k_3\right] \end{aligned} \tag{5}$$

where x_c denotes the middle point of a tapered vessel and (k_1, k_2, k_3) are given in Ref. [5].

3. Formulation of Spectral Finite Element Model

Weak Form in Frequency Domain. Based on the discrete Fourier transform (DFT) theory, we can assume the time histories of $p(x,t)$, $Q(x,t)$, and $f(x,t)$ in the spectral forms as

$$\begin{aligned} p(x,t) &= \frac{1}{N}\sum_{n=0}^{N-1} p_n(x) e^{i\omega_n t}, \\ Q(x,t) &= \frac{1}{N}\sum_{n=0}^{N-1} Q_n(x) e^{i\omega_n t}, \\ f(x,t) &= \frac{1}{N}\sum_{n=0}^{N-1} f_n(x) e^{i\omega_n t} \end{aligned} \tag{6}$$

where $p_n(x)$, $Q_n(x)$, and $f_n(x)$ are the Fourier components of $p(x,t)$, $Q(x,t)$, and $f(x,t)$, respectively; $\omega_n = 2\pi n/T$ (n = 0,1,2,…, N) where T is the period and N is the number of samples in the DFT theory. Substituting Eq. (6) into Eq. (3) yields the governing equations for $Q_n(x)$ and $p_n(x)$ as

$$\begin{aligned} &c_n^2 Q_n'' + \omega_n^2(1-i\eta_n)Q_n + \sigma_{1n} f_n = 0, \\ &c_n^2 p_n'' + \omega_n^2(1-i\eta_n)p_n + \sigma_{2n} g_n = 0 \end{aligned} \tag{7}$$

where $g_n(x)$ are the Fourier components of $g(x, t) = f'(x, t)$ and the following definitions are used.

$$\begin{aligned} &c_n = \sqrt{\frac{a_1^2 + \omega_n^2 a_3^2}{a_1 - a_2 a_3}}, \; \eta_n = \frac{\omega_n^2 a_3 + a_1 a_2}{\omega_n (a_1 - a_2 a_3)}, \\ &\sigma_{1n} = \frac{\omega_n^2 a_3}{a_1 - a_2 a_3}\left\{1 + i\left(\frac{a_1}{\omega_n a_3}\right)\right\}, \\ &\sigma_{2n} = -\frac{a_1(a_1 - i\omega_n a_3)}{a_0(a_1 - a_2 a_3)} \end{aligned} \tag{8}$$

Multiplying Eq. 7(a) by $\delta Q_n(x)$, and Eq. 7(b) by $\delta p_n(x)$, integrating by parts, and finally using the relation $i\omega_n a_0 p_n + Q_n' = 0$ derived from Eq. 3(a) yields the weak forms for the original governing equations. For instance, the weak form for Eq. 7(a) can be derived as follows:

$$\int_0^l c_n^2 Q_n' \delta Q_n' dx - \int_0^l \omega_n^2 (1-i\eta_n) Q_n \delta Q_n dx + \int_0^l \sigma_n f_n \delta Q_n dx + i\omega_n c_n^2 a_0 p_n \delta Q_n \Big|_0^l = 0 \tag{9}$$

Spectral Finite Element Model. To formulate the spectral finite element, we consider the linear homogeneous governing equations reduced from Eq. (7), for instance, as

$$c_n^2 Q_n'' + \omega_n^2 (1-i\eta_n) Q_n = 0 \tag{10}$$

subject to

$$Q_n(0) = Q_{n1}, \; Q_n(l) = Q_{n2}$$

The solution of Eq. (10) can be obtained in terms of the dynamic shape function matrix $\boldsymbol{N}(x, \omega_n)$ and the nodal degrees of freedom (DOFs) $\boldsymbol{Q}_n = \{Q_{n1} \quad Q_{n2}\}^T$ as

$$Q_n(x) = [\boldsymbol{N}(\boldsymbol{x},\boldsymbol{\omega_n})]\{\boldsymbol{Q_n}\} \tag{11}$$

where

$$\begin{aligned} &[\boldsymbol{N}(\boldsymbol{x},\boldsymbol{\omega_n})] \\ &= [\csc(k_n l)\sin(k_n l - k_n x) \quad \csc(k_n l)\sin(k_n x)], \\ &k_n = (\omega_n/c_n)\sqrt{1-i\eta_n} \end{aligned} \tag{12}$$

Substituting Eq. (11) into Eq. (9) gives

$$[\boldsymbol{S}(\boldsymbol{\omega_n})]\{\boldsymbol{Q_n}\} = \{\boldsymbol{f_{1n}}\} + \{\boldsymbol{F_{1n}}\} \tag{13}$$

where

$$\begin{aligned} &[\boldsymbol{S}(\boldsymbol{\omega_n})] = c_n^2 \int_0^l [N']^T [N'] dx \\ &\qquad - \omega_n^2 (1-i\eta_n) \int_0^l [N]^T [N] dx, \\ &\{f_{1n}(Q,p)\} \cong \sigma_{1n} f_n(x_c) \int_0^l [N]^T dx, \\ &\{F_{1n}\} = i\omega_n c_n^2 a_0 \{p_n\} \end{aligned} \tag{14}$$

Similarly, from the weak form for Eq. 7(b), we can derive

$$[\boldsymbol{S}(\boldsymbol{\omega_n})]\{\boldsymbol{p_n}\} = \{\boldsymbol{f_{2n}}\} + \{\boldsymbol{F_{2n}}\} \tag{15}$$

where

$$\begin{aligned} &\{f_{2n}(Q,p)\} \cong \sigma_{2n} g_n(x_c) \int_0^l [N]^T dx, \\ &\{F_{2n}\} = i\omega_n c_n^2 a_0^{-1} \{Q_n\} \end{aligned} \tag{16}$$

4. Numerical Result and Discussion

We consider an ascending aorta as shown in Fig. 1, where r_0 = 1.25 and L = 7 cm. The blood properties are given by ρ = 1.055 g/cm^3 and ν = 0.046 cm^2/s. The blood flow rate and pressure are computed by assuming that the blood flow rate at the inlet (*i.e.*, x = 0) is given by Fig. 2, and the results are displayed in Figs. 3 and 4.

Figure 3 shows the perturbed blood pressure p and blood flow rate Q at x = 3.5 cm obtained by assuming that the blood flow profile is uniform, parabolic, or boundary layered (uniform in the core region and linear in the boundary layer). Though there are not significant differences between different blood flow files, the uniform flow profile seems to provide the largest blood pressure and flow rate while the boundary layered flow profile provides the smallest values.

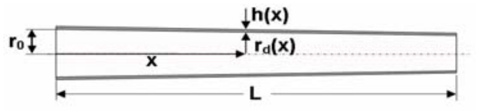

Figure. 1 Geometry of a blood vessel

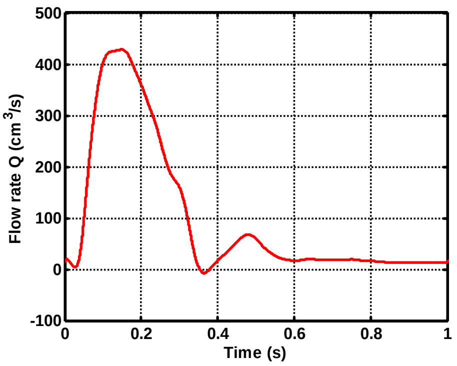

Figure. 2 Flow rate at the inlet of blood vessel.

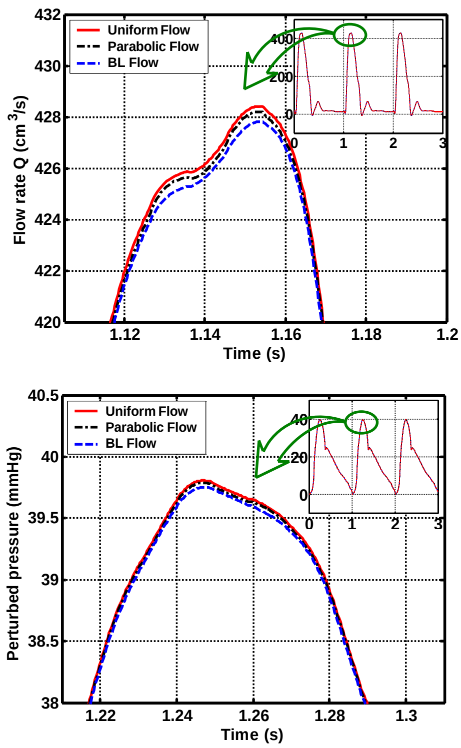

Figure. 3 Blood flow rate and pressure at x = 3.5 cm vs. blood flow profile.

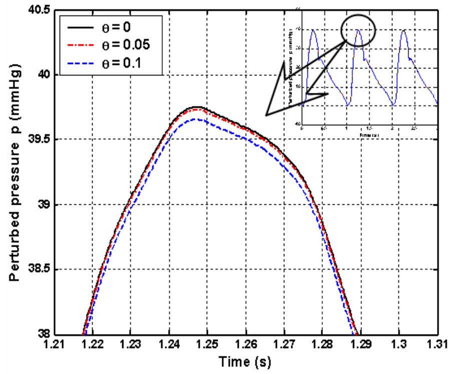

Figure. 4 Perturbed blood pressure vs. blood vessel taper.

Figure 4 shows the effect of the blood vessel taper θ on the perturbed blood pressure at x = 3.5 cm when the blood profile is assumed as the boundary layered blood profile. It is obvious from Fig. 4 that the perturbed blood pressure becomes larger as the blood vessel taper increases.

Though it is not shown here due to the paper length limitation, we also have investigated the blood flow characteristics along the vessel axis. The present spectral finite element model is found to provide the results which accurately capture the wave characteristics of blood flow.

5. Summery

In this paper, one-dimensional spectral finite element model is developed for human blood vessels. The spectral finite element model is formulated by using the frequency-dependent shape functions satisfying the linear governing equations in frequency-domain and the nonlinear terms are all treated as the pseudo-forces. The spectral element model is applied to the ascending aorta to investigate the blood flow rate and pressure for various flow profiles.

References

(1) Wormersly, J. R., 1957, “Oscillatory flow in arteries: the constrained elastic tube as a model of arterial flow and pulse transmission”, Physics in Medicine and Biology 7, pp. 178-187.

(2) Hughes, T. J. R. and Lubliner, J., 1973, “On the one-dimensional theory of blood flow in the larger vessels”, mathematical Biosciences 18, pp. 161-170.

(3) Olufsen, M. S., 1999, “Structured tree outflow condition for blood flow in larger systemic arteries”, American Journal of

Physiology 276, pp. H257-H268.

(4) Wan, J., Steele, B., Spicer, S. A., Strohband, S., Feijoo, G. R., Hughes, T. J. R. and Taylor, C. A., 2002, “A one-dimensional finite element method for simulation-based medical planning for cardiocascular disease”, Computer Methods in Biomechanics and Biomedical Engineering 5(3), pp. 195-206.

(5) Steele, B. N., Wan, J., Ku, J. P., Hughes, T. J. R. and Taylor, C. A., 2003, “In vivo validation of a one-dimensional finite-element method of predicting blood flow in cardiovascular bypass grafts”, IEEE Transactions on Biomedical Engineering 50(6), pp.649-656.

(6) Vignon, I. E. and Taylor, 2004, “C. A. Outflow boundary conditions for one-dimensional finite element modeling of blood flow and pressure waves in arteries”, Wave Motion 39, pp. 361-374.

(7) Formaggia, L., Gerbeau, J. F., 2001, “Nobile, F. and Quarteroni, A., On the coupling of 3D and 1D Navier-Stokes equations for flow problems in compliant vessels”, Computer Methods in Applied Mechanics and Engineering 191, pp. 561-582.

(8) Laganà, K., Dubini, G., Migliavacca, F., Pietrabissa, R. and Pennati, G., Veneziani, A. and Quarteroni, A., 2002, “Multiscale modelling as a tool to prescribe realistic boundary conditions for the study of surgical procedures”, Biorheorogy 39, pp. 359-364.

(9) Doyle, J. F., 1997, Wave Propagation in Structures, Springer, New York